Storage Allocation in Active Distribution Networks Considering Life Cycle and Uncertainty

Tripti Gangwar, *Student Member, IEEE*, Narayana Prasad Padhy, *Senior Member, IEEE*, and Premalata Jena, *Senior Member, IEEE*

***Abstract*—The modern active distribution systems necessitate integrating storage systems, thereby facilitating the large-scale proliferation of photovoltaic (PV) energy resources. This further calls for the optimal planning of energy storage systems, satisfying all the operational and economic constraints. This article describes an exhaustive storage integration method, deeming the life cycle of the battery energy storage, the uncertainty of load and PV output, and the islanded mode of operation of the system. A two-stage mixed-integer linear programming problem is formulated that determines the capacity and the number of discharge cycles of the batteries in the first stage. The lifetime of the battery based on the partial depth of discharge is analyzed in the second stage. Furthermore, the uncertainty and variability of PV and demand are taken into account through probabilistic analysis and time-period clustering. The method is validated on a standard 33-bus radial distribution network for the allocation of distributed lithium-ion batteries. Also, the method's scalability is validated on a practical Indian distribution network and a 141-bus distribution network of metropolitan area of Caracas with distributed PV installations on various nodes.**

***Index Terms*—Battery sizing and location, distributed energy storage, optimal power flow (OPF), uncertainty.**

Nomenclature

Abbreviations

BESS	Battery energy storage system.
CRF	Capital recovery factor.
DG	Distributed generator.
DoD	Depth of discharge.
ESS	Energy storage system.
MILP	Mixed-integer linear programming.
OPF	Optimal power flow.
PV	Photovoltaic.
SoC	State of charge.

Indices and Suffixes

es	Set of battery energy storage.
g	Set of diesel generators.
i, j	Indexes for buses.
ij	Index for branches.
Nb	Number of buses.
pv	Set of PV energy resources.
s	Index for scenarios.
t	Index for time.

Parameters and Inputs

$\alpha_{\text{es}}^{\min}, \alpha_{\text{es}}^{\max}$	Minimum and maximum energy rating to power rating ratio, respectively.
C_E, C_P	Energy rating and power rating cost of battery (\$/kWh and \$/kW), respectively.
$C_{\text{SU}}^g, C_{\text{SD}}^g$	Startup and shutdown cost of diesel generator (\$), respectively.
g_{ij}, b_{ij}	Conductance and susceptance of branch ij ($\mho$), respectively.
IR	Hourly PV irradiation (W/m^2).
$\text{IR}^c, \text{IR}^{\text{std}}$	Certain irradiation point (150 W/m^2) and standard PV irradiation (1000 W/m^2), respectively.
MP_t	Market price (\$/kW).
$P_{\text{es}}^{\text{dch,max}}, P_{\text{es}}^{\text{ch,max}}$	Storage discharging and charging maximum power limits (kW), respectively.
$P_{i,s,t}^{\text{demand}}$	Active load demand at each bus for each hour (kW).
$P_{\text{pv},s,t}$	Hourly PV output (kW).
$Q_{i,s,t}^{\text{demand}}$	Reactive load demand at each bus for each hour (kVAR).
R_{ij}, X_{ij}	Resistance and reactance of branch ij (Ω), respectively.
VOLL	Value of lost load (\$/kWh).
$\text{Cf}_{\text{es,pc}}, \text{Cf}_{\text{DoDmax}}$	Number of cycles to failure for partial and maximum DoD values (given by manufacturer), respectively.
$\eta_{\text{ch}}, \eta_{\text{dch}}$	BESS charging and discharging efficiency (%), respectively.

Manuscript received 9 October 2021; revised 11 February 2022; accepted 31 March 2022. Date of publication 14 April 2022; date of current version 8 November 2022. This work was supported by the Department of Science and Technology (DST), India smart grid research initiatives, under Grant D-SIDES:DST-1237 EED, Grant ZED-I: DST-1161-APD, Grant UI-ASSIST: IUS-1132-EED, and Grant ID-EDGe: DST-1390-EED. Paper no. TII-21-4437. *(Corresponding author: Tripti Gangwar.)*

The authors are with the Department of Electrical Engineering, Indian Institute of Technology, Roorkee 247667, India (e-mail: tripti.gangwar5@gmail.com; nppeefee@gmail.com; premalata.jena@ee.iitr.ac.in).

Color versions of one or more figures in this article are available at https://doi.org/10.1109/TII.2022.3167382.

Digital Object Identifier 10.1109/TII.2022.3167382

1551-3203 © 2022 IEEE. Personal use is permitted, but republication/redistribution requires IEEE permission.
See https://www.ieee.org/publications/rights/index.html for more information.

e-tarjome.com

Authorized licensed use limited to: The University of Toronto. Downloaded on December 17,2022 at 09:05:05 UTC from IEEE Xplore. Restrictions apply.

$P_{\text{es}}^{\text{dch,max}}, P_{\text{es}}^{\text{ch,max}}$	Maximum charging and discharging power limits, respectively.
$P_{\text{rated}}^{\text{pv}}$	Rated capacity of installed PV systems.
Variables	
$\Delta V_{i,s,t}, \Delta V_{j,s,t}$	Voltage deviation at bus i and bus j (kV), respectively.
$\theta_{ij,s,t}$	Angle difference of branch ij (radians).
$E_{\text{es},s,t}$	Stored energy in a battery at time "t" (kWh).
$\text{Er}_{\text{es}}, \text{Pr}_{\text{es}}$	Energy and power capacity of battery (kWh and kW), respectively.
$LCP_{i,s,t}$	Active load curtailment at bus i during islanding (kW).
$LCR_{i,s,t}$	Reactive load curtailment at bus i during islanding (kVAR).
Ncc_{es}	Number of complete cycles of battery.
Npc_{es}	Number of partial cycles of battery.
$P_{\text{es},s,t}^{\text{dch}}, P_{\text{es},s,t}^{\text{ch}}$	Storage discharging and charging power (kW), respectively.
$P_{g,s,t}$	Power output of diesel generator (kW).
$P_{ij,s,t}$	Active power flow from bus i to bus j (kW).
$P_{s,t}^{\text{grid}}$	Active power input from grid (kW).
$\text{PL}_{ij,s,t}$	Active power loss of branch ij (kW).
$Q_{ij,s,t}$	Reactive power flow from bus i to bus j (kVAR).
$Q_{s,t}^{\text{grid}}$	Reactive power input from grid (kVAR).
$QL_{ij,s,t}$	Reactive power loss of branch ij (kVAR).
$U_{\text{es},s,t}^{c}, U_{\text{es},s,t}^{d}$	Charging and discharging status of battery, respectively.
$u_{s,t}^{g}$	Diesel generator operating state.
$\text{DoD}_{\text{es},s,t}$	Hourly depth of discharge of battery.
$\text{DoDpc}_{\text{es},s,t}$	Hourly depth of discharge of of each partial cycle of battery.
V_i, V_j	Voltage magnitude at bus i and bus j (kV), respectively.

I. Introduction

A. Motivation and Bibliographic Review

SMART grid is a gratuity to the consumers and the stakeholders involved in the electric grid's generation, transmission, and distribution sections. It includes the complete modernization of the power system with smart meters, automation devices, intelligent monitoring, demand-side management, and self-healing capability schemes. Along with these activities, generation units are set up in the distribution section, i.e., nearer to the consumer premises, to reduce the transmission losses. This shift of the electric grid from a passive network to a bidirectional active network is due to the small generators being set up in the distribution grid known as distributed/decentralized generation. These distributed generators (DGs) mainly generate energy using renewable energy resources, such as photovoltaic (PV), wind, biomass, tidal, etc., as they are clean sources of energy and promote sustainable development. However, the intermittent nature and excess penetration of these resources pose problems, such as reverse power flow, voltage fluctuations, increase in losses, harmonic distortion, and instantaneous matching of demand and supply [1], [2]. Although integrating storage systems in the distribution network can help alleviate the aforementioned problems if allocated optimally. Also, India's target of 40-GW PV rooftop installations by the year 2022 and the declining cost of batteries will provide a fillip to the installation of energy storage systems (ESSs) [3]. Therefore, an ESS can be seen as a game changer in the ever-changing power system paradigm and can serve multiple ranges of benefits. To achieve these benefits, methods for optimal sizing, allocation, and operation of ESSs are required.

The optimal location and sizing of storage have been addressed extensively in the literature, taking various parameters with diverse objectives and constraints. In the literature, peak management, voltage and frequency regulation, minimizing renewables stochasticity, and back up are the main functions of a storage system [2]. To serve these applications, planning of energy storage in a distribution system is necessary. The planning problem in an active distribution network is the mixed-integer nonlinear programming (NLP) problem, which is computationally intractable. Various approaches, such as heuristics, mathematical optimization, and artificial intelligence, are reviewed [1], [2], [4]. Santos *et al.* [5] and Aien and Fotuhi-Firuzabad [6] formulated the problem as an optimal power flow (OPF) to determine the location and size of storage systems. These formulations consist of a nonconvex power flow equation that requires certain relaxations and increases the computational burden. Also, second-order cone programming-based OPF relaxation models used in some works may face difficulties in reverse power flow. The technique explained in [6] aimed at finding the most favorable storage configuration for preventing over-voltage and under-voltage in a distribution network. The use of heuristics for the location and OPF convex relaxation framework for sizing minimizes the total deployment cost of storage. The technical definition of heuristic signifies "it as a simple procedure that helps find answers to difficult questions though often imperfect". Thus, the planning problem's formulation as a heuristic procedure does not guarantee global optima. Lyzwa *et al.* [7] proposed an energy mix model, particularly for investment planning using mixed-integer linear programming (MILP). Moreover, the traditional planning models have not yet included the range of grid services, provided by energy storage devices and their life cycle assessment. They are not designed to identify the benefits of storage in terms of grid flexibility [4]. With the increase in the proliferation of PV rooftop installations, researchers' focus is shifted to energy storage optimization, including uncertainty, islanded operation, and the life cycle of the facility. The lifespan of batteries was considered in [8] by formulating two objective functions representing energy losses and the total investment cost of the DG and battery installations. It also considers factors, such as the temperature and depth of discharge (DoD) affecting the lifespan of the battery. Battery aging is a nonlinear process that depends on stress factors, such as time, temperature, state of charge (SoC), DoD, and number of charging/discharging cycles [9]. Antoniadou-Plytaria *et al.* [10] modeled the cycling and calendar aging of the battery by considering a degradation cost model. Also, Shen *et al.* [11]

Authorized licensed use limited to: The University of Toronto. Downloaded on December 17,2022 at 09:05:05 UTC from IEEE Xplore. Restrictions apply.

TABLE I
TAXONOMY OF THE REVIEWED LITERATURE

S no.	Ref.	Formulation method	Uncertainty	Islanded mode	Battery life-cycle	Solution technique	Remarks
1.	[5]	AR-OPF	✓	✗	✓	Benders decomposition	Fixed life of the battery with a limit to the number of cycles
2.	[6]	SDP relaxation OPF	✓	✗	✗	Heuristic and CVX (SeDuMi solver)	Uncertainty through different demand and generation profiles
3.	[4]	AC-PF linear programming	✓	✗	✓	Benders decomposition	Min. of degradation cost, a standard expression not yet defined
4.	[8]	Multi-objective	✓	✗	✓	Heuristic (NSGA-II)	Battery parameters dependency and local optimality
5.	[11]	Multi-objective	✗	✗	✓	DIRECT algorithm	Battery cycle life estimation
6.	[12]	Non-linear objective	✗	✗	✓	Not specified	Fixed battery profile input
7.	[14]	Unit commitment	✓	✓	✗	Heuristic (particle swarm optimization)	Probabilistic method, however battery lifetime ignored
8.	[15]	AC-OPF	✓	✗	✗	Heuristic and S-MILP	Battery lifetime ignored
9.	Proposed method	AC-OPF	✓	✓	✓	MILP (GUROBI solver)	Partial cycles along with complete cycles of battery for lifetime estimation

✓ = Considered; ✗=Not considered

illustrated a cycle life estimation model of battery using battery DoD, temperature, and current rate. In [12], the battery's degradation was taken into account with a fixed load profile for the battery and only one continuous variable with a nonlinear objective function. The method proposed in [13] considered the impact of a prefixed maximum DoD on expected lifetime and fixed inputs for load demand and renewables. However, many of the works have not yet considered lifetime estimation using partial and complete charging/discharging cycles. The uncertainty is captured by using a probabilistic unit commitment technique [14]. Santos *et al.* [15] formulated a multistage distribution expansion planning problem as a MILP to determine the optimal location and sizing of distributed energy resources. The uncertainty of PV and load in this article is quantified using multiscenario modeling. Moreover, many approaches are used in the literature for capturing the uncertainty of PV and load techniques, such as scenario generation and reduction and probabilistic and possibilistic analysis [16]–[18].

However, the main challenge for integrating storage in the distribution network is its optimal allocation by considering the various factors, such as characteristics of different technologies, DoD, charging and discharging cycles impact on life cycle, distributed or aggregated placement, [19] etc.

B. Aim and Contribution

Corresponding to the abovementioned literature survey, there is a growing interest in the optimal planning of storage systems using stochastic formulation, distributed placement, etc. Several applications to distributed energy storage are also well-presented in the literature [1], [2]. However, there are certain gaps from the following perspectives.

1) The handling of the lifetime of the battery is overlooked. It is inferred from Table I that either fixed lifetime of battery is considered or lifetime is estimated using only complete cycles of discharge.
2) The islanded mode of operation increases the sizes of storage required [14]. Different sizes for islanded and grid-connected mode are given in literature, which is practically infeasible.

Considering the abovementioned perspectives, this article aims to find the optimal location and size of batteries in a distribution network to minimize the voltage fluctuations when there is a high penetration of PV-based DGs. Besides, the optimally located batteries will reduce the losses, and also help in smoothing the fluctuating output of PV. The sizing problem proposed here is unique, which includes the partial cycles of discharging of batteries for lifetime assessment. The planning problem proposed here can also be used as a subproblem in the case of scheduling, as it uses a linearized ac-OPF where losses are modeled using the special-ordered set of type-2 (sos2) model. The main contributions of this article are as follows.

1) Distributed battery ESS (BESS) planning, including candidate buses placement, islanded and grid-connected mode of operation, the uncertainty of PV and loads, and estimation of battery's operating life cycle, is proposed for an active distribution system.
2) The proposed approach considers estimating battery life based on partial and complete discharging cycles and the number of cycles to failure dependence on the upper limit of DoD.
3) A linearized ac-OPF-based MILP model is described in this article. The model's computational intractability is reduced, and accuracy is increased by modeling the line losses using sos2-based approximation.
4) Scenario-based modeling of PV and demand, as uncertainty of loads and renewable energy resources will affect the optimal allocation decision.

C. Article's Framework

The rest of this article is organized as follows: Section II briefly describes the modeling and problem formulation with a list of all the constraints and the objective function. Besides, Section III illustrates proposed method and the modeling of uncertain and variable parameters. Section IV presents the validation of the work. Finally, Section V concludes this article.

Authorized licensed use limited to: The University of Toronto. Downloaded on December 17,2022 at 09:05:05 UTC from IEEE Xplore. Restrictions apply.

II. Modeling and Problem Formulation

A. Brief Outline of the Problem

This article's general objective is to identify connection buses and capacity for BESS to minimize the investment and operation cost of a radial active distribution system. Here, the problem is formulated by identifying the candidate buses suitable for placing the storage devices in the system. A comparative study has been carried out based on the result of candidate bus placement, and taking into account all the buses (except the slack bus) of the system for BESSs placement. Since the planning and operation of energy storage will be affected by uncertainty, operating mode (islanded or grid-connected mode), and battery lifetime, the key contribution of the proposed approach lies in incorporating all these factors. Furthermore, this article considers a linearized ac-OPF-based MILP model for representing the distribution network system and BESS. Also, an algorithm is formulated in the second stage to determine the number of cycles of BESS. This takes into account the partial DoD values and the maximum DoD for the estimation of the battery life cycle. The uncertainty of load and PV is addressed by generating scenarios. A time-period clustering method is used for selecting the representative day to retain the chronological sequence for analyzing the battery operation throughout a day. The proposed method is tested on a PV penetrated 33-bus radial distribution system. To show the scalability of the method, a 115-node practical Indian distribution network and a 141-bus distribution network of metropolitan area of Caracas are used. The constraints and the objective of the formulated problem are given in the following section.

B. Operational Equations

1) Network Constraints:

a) *Power Flow Equations:* The ac power flow equations [see (1) and (2)] representing active and reactive power flow through branch ij are nonconvex and nonlinear. Therefore, using these equations in distribution system planning is extremely undesirable.

$$P_{ij} = V_i^2 g_{ij} - V_i V_j \left(g_{ij}\cos\theta_{ij} + b_{ij}\sin\theta_{ij}\right) \quad (1)$$

$$Q_{ij} = -V_i^2 b_{ij} + V_i V_j \left(b_{ij}\cos\theta_{ij} - g_{ij}\sin\theta_{ij}\right). \quad (2)$$

Two practical assumptions are made to simplify the aforementioned equations to be linear and solved using a linear programming approach. The first assumption is related to nodal voltage magnitudes, which are assumed close to the rated voltage in a distribution network, as given in (3). Also, the small voltage angle difference of a branch ij leading to the approximation of $\sin\theta_{ij} \approx \theta_{ij}$ and $\cos\theta_{ij} \approx 1$ is considered. However, this assumption is valid only if the active power flow dominates the apparent power flow [20].

$$V_i = 1 + \Delta V_i \quad \text{where } \Delta V^{\min} \le \Delta V_i \le \Delta V^{\max}. \quad (3)$$

The values of $\Delta V^{\min}$ and $\Delta V^{\max}$ in this article are considered as -0.05 and $+0.05$ per unit, respectively [21].

On substituting the abovementioned assumptions and neglecting the product of small variables (θ_{ij}, ΔV_i, and ΔV_j), the linearized ac power flow through a branch ij is expressed as

$$P_{ij,s,t} = (\Delta V_{i,s,t} - \Delta V_{j,s,t}) g_{ij} - \theta_{ij,s,t} b_{ij} \quad (4)$$

$$Q_{ij,s,t} = -(\Delta V_{i,s,t} - \Delta V_{j,s,t}) b_{ij} - \theta_{ij,s,t} g_{ij}. \quad (5)$$

b) *Nodal Power Balance:* For all time instants, the load should be satisfied at each and every node. Applying the Kirchhoff's current law at each node, i.e., the sum of all injections is equal to the sum of all withdrawals, and is given as

$$P^{\text{grid}}_{s,t} + P_{\text{pv},s,t} + LCP_{i,s,t} + P^{\text{dch}}_{\text{es},s,t} - P^{\text{ch}}_{\text{es},s,t} = P^{\text{demand}}_{i,s,t} + \sum_{\text{out},j\in\text{Nb}} P_{ij,s,t} - \sum_{\text{in},j\in\text{Nb}} P_{ij,s,t} + \sum_{\text{out},j\in\text{Nb}} 0.5 * PL_{ij,s,t} + \sum_{\text{in},j\in\text{Nb}} 0.5 * PL_{ij,s,t} \quad (6)$$

$$Q^{\text{grid}}_{s,t} + LCR_{i,s,t} = Q^{\text{demand}}_{i,s,t} + \sum_{\text{out},j\in\text{Nb}} Q_{ij,s,t} - \sum_{\text{in},j\in\text{Nb}} Q_{ij,s,t} + \sum_{\text{out},j\in\text{Nb}} 0.5 * QL_{ij,s,t} + \sum_{\text{in},j\in\text{Nb}} 0.5 * QL_{ij,s,t}. \quad (7)$$

Unlike the nonlinearized ac power flow, which captures the losses inherently, the linearized approach presented here relinquishes this property. Therefore, the losses in the lines need to be modeled separately.

c) *Modeling of Losses:* In an ac power flow model, the losses can be modeled and expressed as

$$PL_{ij,s,t} = P_{ij,s,t} + P_{ji,s,t}. \quad (8)$$

However, due to the linearization method, the power flow through the same line when measured at bus j is

$$P_{ji,s,t} = -(\Delta V_{i,s,t} - \Delta V_{j,s,t}) g_{ij} + \theta_{ij,s,t} b_{ij}. \quad (9)$$

Therefore, the losses however modeled in terms of the quadratic active and reactive power flows in each feeder [22] are given by

$$PL_{ij,s,t} = (P^2_{ij,s,t} + Q^2_{ij,s,t}) R_{ij} \quad (10)$$

$$QL_{ij,s,t} = (P^2_{ij,s,t} + Q^2_{ij,s,t}) X_{ij}. \quad (11)$$

The abovementioned quadratic expressions of active and reactive power flow are modeled by creating a mixed-integer sos2-based approximation [23].

2) Energy Storage Constraints:

The equations given in this section are used for modeling the battery energy storage to be optimally allocated. The given equations are generalized to be used for any energy storage device [15], [5]. However, this article considers batteries as the most captivating storage systems for low-voltage distribution networks due to their sufficient energy and power rating. The various constraints with a brief clarity on the equations are given as follows.

Authorized licensed use limited to: The University of Toronto. Downloaded on December 17,2022 at 09:05:05 UTC from IEEE Xplore. Restrictions apply.

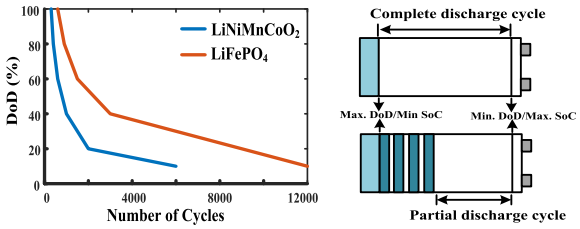

(a) (b)

Fig. 1. (a) DoD versus number of cycles for lithium-ion batteries. (b) Illustration for the partial and complete cycle.

The absolute SoC is the total amount of energy stored in the battery at time t expressed as

$$E_{\text{es},s,t} = E_{\text{es},s,(t-1)} - \Delta t \left(\frac{P^{\text{dch}}_{\text{es},s,t}}{\eta_{\text{dch}}} - P^{\text{ch}}_{\text{es},s,t} \eta_{\text{ch}} \right). \quad (12)$$

Also, this energy balance is validated at the end of every time interval. Expression in (13) is added to prevent simultaneous charging and discharging of batteries

$$U^{c}_{\text{es},s,t} + U^{d}_{\text{es},s,t} \leq 1. \quad (13)$$

The initial and final energy stored level is maintained the same with half of the energy capacity of the battery as

$$E_{\text{es}}(1) = E_{\text{es}}(t) = 50\% Er_{\text{es}} \quad (14)$$

where t is the end of the day, i.e., 24 h.

The charging and discharging power of the battery is limited to a maximum charging and discharging in the battery to prevent overcharge and overdischarge. This will aid in the life cycle improvement of the battery as overcharging and overdischarging can affect the lifetime of the battery.

$$\begin{aligned} 0 \leq P^{\text{dch}}_{\text{es},s,t} &\leq U^{d}_{\text{es},s,t} * P^{\text{dch,max}}_{\text{es}} \\ 0 \leq P^{\text{ch}}_{\text{es},s,t} &\leq U^{c}_{\text{es},s,t} * P^{\text{ch,max}}_{\text{es}}. \end{aligned} \quad (15)$$

The power and energy rating of the batteries are correlated with respect to the minimum and maximum discharge time, which is assumed as 0 and 4 h, respectively, in this article. Hence, the upper and lower bound to the energy rating of the batteries are given by

$$\alpha^{\text{min}}_{\text{es}} * Pr_{\text{es}} \leq Er_{\text{es}} \leq \alpha^{\text{max}}_{\text{es}} * Pr_{\text{es}} \quad (16)$$

a) *Depth of Discharge:* DoD and the number of charging/discharging cycles are the parameters selected for analyzing the cycle life of lithium-ion batteries. The number of charging/discharging cycles or cycle life depends on the normally used capacity of the battery. Also, the number of cycles of a battery decrease with an increase in the DoD Fig. 1(a) shows the variation of cycles to failure with DoD for two different compositions of lithium-ion batteries. It can be inferred that the battery has more useful cycles if it is regularly discharged at less DoD value instead of less frequent draining of battery to maximum DoD. It is also evident that there is no need to discharge the battery completely before recharging. Nonetheless, most of the published literature does not distinguish between partial and complete cycles (maximum DoD) for evaluating the battery's life cycle. Fig. 1(b) shows the difference between the complete and partial discharging cycle of a battery. The lithium-ion batteries work on charge cycles, and one full cycle will be defined if 100% of the battery capacity is utilized, but not necessarily from one charge. Hence, the DoD evaluation is considered in the second stage of the method with known energy ratings of the batteries (obtained from first stage results) to evaluate the lifetime based on the number of cycles to failure provided by the manufacturer. Here, the DoD of each partial cycle is evaluated using the expressions [see (17) and (18)], and then the battery's lifetime is assessed in years.

$$\text{DoD}_{\text{es},s,t} = 1 - \frac{E_{\text{es},s,t}}{Er_{\text{es}}} \quad (17)$$

$$\text{DoDpc}_{\text{es},s,t} = \text{DoD}_{\text{es},s,t} - \text{DoD}_{\text{es},s,t-1}. \quad (18)$$

b) *Number of Cycles:* The following formulation is used to determine the number of partial cycles of a battery. One partial cycle is counted when the discharging status of the battery changes from 1 to 0 and again to 1. The equations for estimating the number of cycles as modeled in "YALMIP" are given as follows:

$$\text{Case}_1, [(U^{d}_{\text{es},t} - U^{d}_{\text{es},(t-1)}) = 1 \Rightarrow \text{Npc}_{(\text{es},t)} = 1] \quad (19)$$

$$\text{Case}_2, [(U^{d}_{\text{es},t} - U^{d}_{\text{es},(t-1)}) = 0 \Rightarrow \text{Npc}_{(\text{es},t)} = 0] \quad (20)$$

$$\text{Case}_3, [(U^{d}_{\text{es},t} - U^{d}_{\text{es},(t-1)}) = -1 \Rightarrow \text{Npc}_{(\text{es},t)} = 0] \quad (21)$$

$$\text{and} \;\; \text{Case}_1 + \text{Case}_2 + \text{Case}_3 = 1. \quad (22)$$

c) *Evaluation of BESS Lifetime:* The BESS lifetime can be estimated by calculating the degradation due to partial and complete cycles with the cycles to failure at each DoD_{pc}. The manufacturer provides the number of cycles to failure at each DoD. Hence, the lifetime of the battery is based on the Miner's rule for fatigue damage [24]. The following expression evaluates the lifetime based on the degradation of the battery due to the partial and complete number of cycles performed for each DoD level:

$$\text{ES}_{\text{Lifetime}} = \frac{1}{\sum_{\text{DoD}_{\text{pc}}} \frac{\text{Npc}_{\text{es}}}{Cf_{\text{es,pc}}}}. \quad (23)$$

The lifetime evaluated from (23) is then utilized to compute a limit to the number of complete cycles of BESS placed at each node. The number of cycles per day of the battery is then limited by the constraint expressed as

$$\text{Ncc}_{\text{es}} \leq \frac{Cf_{\text{DoDmax}}}{\text{ES}_{\text{Lifetime}}}. \quad (24)$$

Authorized licensed use limited to: The University of Toronto. Downloaded on December 17,2022 at 09:05:05 UTC from IEEE Xplore. Restrictions apply.

Here, for each BESS, the number of complete cycles for each year is limited to eliminate the replacement cost from the objective function.

C. Objective Function

The objective of the proposed planning framework is designed to minimize the investment and operation and maintenance cost of the system subjected to the abovementioned constraints. This article considers lithium-ion batteries as the storage technology to be deployed in the test network due to the high energy density and an increased number of cycles to failure with fewer maintenance requirements. The values of energy rating and power rating cost with 4 h of discharging are taken from [25]. Also, the fixed operation and maintenance cost is selected as 2.5% of power rating capacity [25]. A capital recovery factor (CRF) with a 4% rate of interest and eight years of a lifetime is multiplied with the cost parameters for normalization. For the grid-connected mode of the system, the objective function is formulated as

$$\begin{gathered}\text{OF} = \text{CRF}((C_E * \textstyle\sum_{\text{es}} Er_{\text{es}} + C_P * \sum_{\text{es}} Pr_{\text{es}}) + \\ \textstyle\sum_{s,t} \text{MP}_{s,t} * P_{s,t}^{\text{grid}} + 0.025 * C_P * \sum_{\text{es}} Pr_{\text{es}} \\ \text{CRF} = \frac{r(1+r)^l}{(1+r)^l - 1}.\end{gathered} \tag{25}$$

However, the islanded mode of the system is supported by diesel generators for minimizing the amount of load curtailment. Here, the objective function for operation and maintenance is designed to minimize the investment and operation cost and the amount of load curtailment.

$$\begin{gathered}\text{OF} = u_{s,t}^g F_g(P_{s,t}^g) + \text{SU}_{s,t}^g + \text{SD}_{s,t}^g + \text{CRF} * (C_E * \textstyle\sum_{\text{es}} \\ Er_{\text{es}} + C_P * \textstyle\sum_{\text{es}} Pr_{\text{es}} + 0.025 \times C_P * \sum_{\text{es}} Pr_{\text{es}}) + \\ \textstyle\sum_{s,t} (LCP_{i,s,t} + LCR_{i,s,t})\text{VOLL} \\ \text{SU}_{s,t}^g = C_{SU}^g \max(u_{s,t}^g - u_{s,t-1}^g, 0) \\ \text{SD}_{s,t}^g = C_{SD}^g \max(u_{s,t-1}^g - u_{s,t}^g, 0).\end{gathered} \tag{26}$$

All the abovementioned constraints and objective are used to formulate an ac-OPF solution technique for the proposed problem. The proposed algorithm for finding the optimal solution to the problem is explained in the following section.

III. Proposed Algorithm

A brief description of the problem is given in the previous section, and the flow chart of the algorithm for the total storage allocation problem in a distribution network is shown in Fig. 2. It shows that the formulated optimal sitting and sizing problem is divided into two stages with input data of load, network, candidate buses, and other storage and network parameters. The scenarios and the candidate buses result is used as an input to the stage 1, which solves an ac-OPF algorithm with (3)–(7), (10)–(17), and (19)–(22) as constraints and (25)–(26) as objective. Stage 1 results in the optimal sizes of the batteries with the discharging and charging profile. This size of the distributed battery energy storage in the system is then used to determine the effect of DoD on the cycle life of the batteries. The stage 2 calculates the number of cycles and the lifetime of the battery in

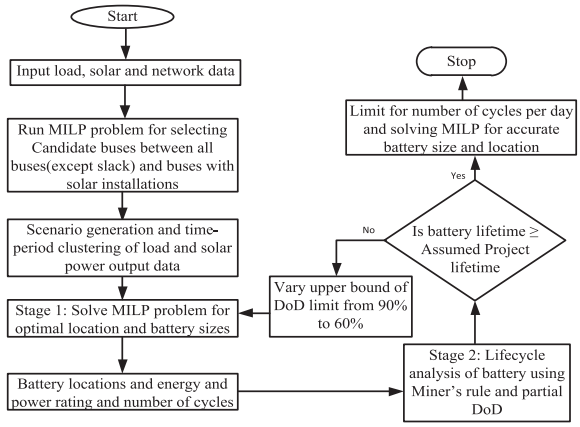

Fig. 2. Flow chart of the proposed optimization approach.

years by using partial and complete DoD values in the Miner's rule. The maximum DoD is varied from 60% to 90% and the BESS is evaluated for lifetime variation with respect to change in DoD. This article uses fractional DoD values obtained in (18) to determine the cumulative degradation of the batteries. The number of complete cycles per day given in (24) are then limited according to the assumed project lifetime of 8 years. Also, the planning problem is affected by uncertainty of demand and renewables, the scenario-based probabilistic method is used for uncertainty modeling. The method used for uncertainty and variability analysis is explained in the subsequent section.

A. Uncertainty and Variability Analysis

With the proliferation of renewable energy resources in the distribution network, uncertainty, and variability of these resources should also be considered during analysis. The PV output considered in the problem is both variable and uncertain due to the variation in irradiation. Also, the load demand for the system is varying with time. One year hourly variation of demand is considered, which follows the IEEE-RTS load profile, as given in [26]. The PV irradiation data of 1 year are obtained from [27]. To reduce the formulated MILP problem's computational intractability, the 1-year data of load demand and PV irradiation are divided into four seasons. A representative day of each season is obtained from the hierarchical clustering method using Ward's linkage [28]. The method used in this article retains the chronological order of the data, which is not preserved using other clustering techniques, such as K-nearest neighbor. Based on the methods reviewed in the literature and to deal with forecast errors for uncertainty modeling, probabilistic modeling of demand and PV irradiation are carried out. A normal and beta probability distribution function is selected to mimic the variable and uncertain power demand and PV irradiation nature [29].

$$\begin{gathered}f(IR : a_\beta, b_\beta) = \frac{\Gamma(a_\beta + b_\beta)}{\Gamma a_\beta \Gamma b_\beta}(IR)^{(a_\beta - 1)}(1 - IR)^{(b_\beta)} \\ a_\beta = \left[\frac{(1-\mu)\mu}{\sigma} - 1\right], b_\beta = (1-\mu)\left[\frac{(1-\mu)\mu}{\sigma} - 1\right]\end{gathered} \tag{27}$$

Authorized licensed use limited to: The University of Toronto. Downloaded on December 17,2022 at 09:05:05 UTC from IEEE Xplore. Restrictions apply.

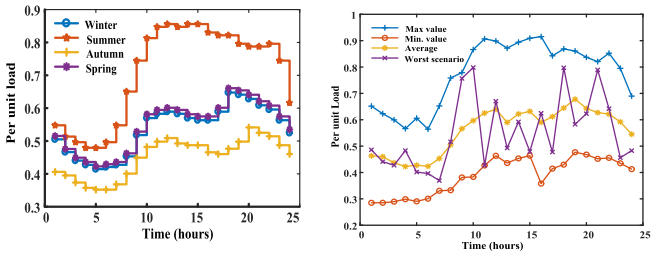

(a) (b)

Fig. 3. (a) Representative days load variation. (b) Max., min., average, and worst scenarios of load data.

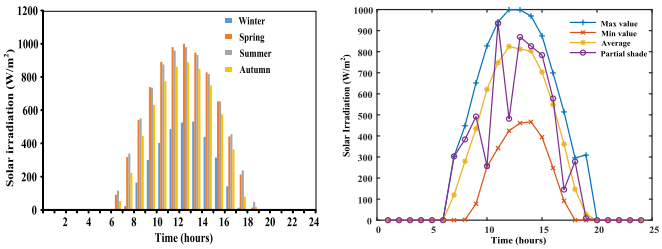

(a) (b)

Fig. 4. (a) PV data scenarios. (b) Max., min., average, and worst scenarios of solar data.

$$f(\text{demand}) = \frac{1}{\sqrt{(2\pi\sigma^2)}} e^{\frac{-1}{2}\left(\frac{\text{demand}-\mu}{\sigma}\right)^2}. \tag{28}$$

The PV power output as a function of irradiation is then calculated using the following expression:

$$P_{\text{pv}} = \begin{cases} P^{\text{pv}}_{\text{rated}} \frac{\text{IR}^2}{\text{IR}^{\text{std}}\text{IR}^c}, & \text{if } 0 \le \text{IR} \le \text{IR}^c \\ P^{\text{pv}}_{\text{rated}} \frac{\text{IR}}{\text{IR}^{\text{std}}}, & \text{if } \text{IR}^c \le \text{IR} \le \text{IR}^{\text{std}} \\ P^{\text{pv}}_{\text{rated}}, & \text{if } \text{IR}^{\text{std}} \le \text{IR} \end{cases}.$$

Thus, four base case days representing each season: 1) winter; 2) spring; 3) summer; and 4) autumn, in demand and PV irradiation are considered, as shown in Figs. 3(a) and 4(a), respectively. A total of 1000 scenarios comprising all the seasonal variations were generated by taking the base case as mean value and a standard deviation of 5% for both demand and PV irradiation considering the forecast errors. The 1000 scenarios will lead to computational burden on the solver, and hence, we have reduced the number to 50 scenarios using the k-means clustering technique. The worst case scenarios, such as partial cloudy days, low value of demand, and islanding condition, are also considered in the formulation. The representative days of each of the four seasons and the scenarios for load and PV irradiation are given in Figs. 3 and 4, respectively.

IV. Results and Discussion

This section demonstrates the competency of the proposed method using three case studies. The first is a standard 33-bus radial distribution system. Furthermore, to show the proposed method's scalability, a modified practical IIT Roorkee campus and a 141-bus radial distribution network are selected. The

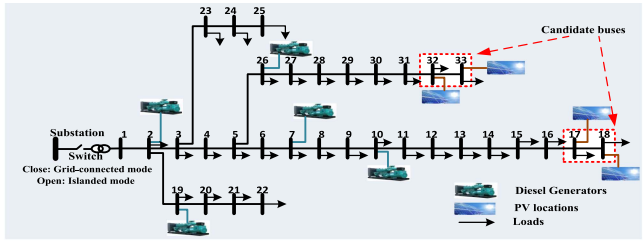

Fig. 5. Single line diagram of 33-bus radial distribution network with PV and DG locations.

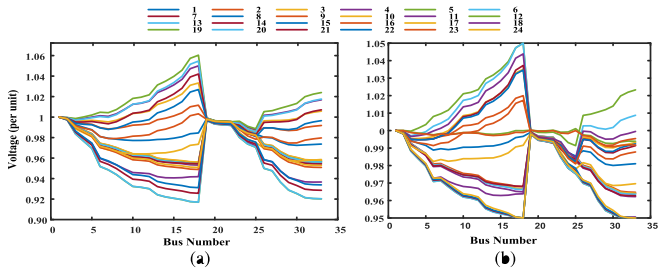

Fig. 6. Voltage variations for 24 h and at the respective buses: (a) without BESS; (b) with BESS allocation.

problem for all the case studies is solved using GUROBI 9.0.1 solver via YALMIP (the MATLAB 2019b interface) on a desktop PC with 16 GB RAM and Intel(R) Core(TM) i7-8700 CPU @ 3.20 GHz [23]. Another consideration in this article is the deployment of batteries is to be achieved in the first year of the planning period; thus, annualized modeling and simulation are performed. It is different from the multiperiod planning of bulk power systems, where new components are added in additional years. Moreover, the distributed BESSs are planned for the existing portfolio of the network.

A. Test System A: 33-Bus Radial Network

The 33-bus radial distribution system [22] is modified by penetrating PV at buses 17, 18, 32, and 33 with a penetration level of 80%. The data of loads and DGs are procured from [30]. The single line diagram with PV, diesel generators', and candidate buses positions at respective buses is shown in Fig. 5.

A 24-h backward/forward load flow is performed on the PV integrated system to observe the voltage violation due to PV penetration, and the results are shown in Fig. 6(a). However, after battery integration through the formulated method, the voltage variations over the 24 h at respective buses is within limits of 0.95–1.05 per unit, as shown in Fig. 6(b). Also, the sudden change in the voltage at hours 5, 11, and 23 is due to the islanding of the system. Thus, deploying BESSs with PV helps better utilize the system by storing surplus power and discharging it later.

1) Candidate Buses Selection: A battery can be connected in a distribution system primarily in most buses due to the less environmental and nontechnical constraints. Despite this, electrical constraints, such as power flow, losses, and voltage

Authorized licensed use limited to: The University of Toronto. Downloaded on December 17,2022 at 09:05:05 UTC from IEEE Xplore. Restrictions apply.

TABLE II
SELECTION OF CANDIDATE BUSES

Parameters	All buses(except slack)	PV buses
Optimal buses	14, 17, 18, 31, 32, 33	17, 18, 32, 33
Best Objective value($)	196102.4	195900
Total Power losses	0.15 MW	0.15 MW
Total Energy and power rating	6.93 and 1.73 MW	6.5 and 1.63 MW

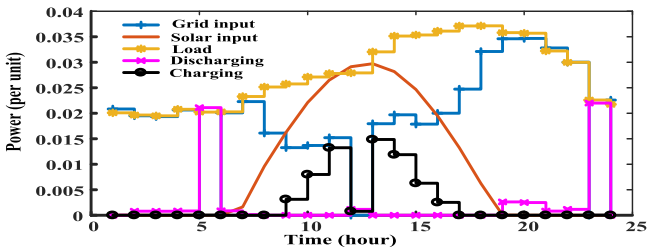

Fig. 7. Variation of grid power, total charging, and discharging of batteries, PV, and load with islanding at fifth, 12th, and 23rd hour.

TABLE III
OBTAINED ENERGY AND POWER RATING

Bus no.	Energy rating (MWh)	Power rating (MW)
17	2.53	0.63
18	0.71	0.17
32	4.00	1.00
33	0.76	0.19

regulation, affect the optimal location of batteries. It is also proved that PV and battery work well in-tandem. A comparison for selecting the candidate buses is made between all the system buses (except slack bus), and PV-connected buses for a grid-connected mode deterministic formulated problem. The results are displayed in Table II, and the buses with PV connections with less objective value were selected as candidate buses for the installation. Furthermore, this will result in cost-saving related to land acquisition, site preparation, sharing of switch-gear, transformers, interconnection, installation labor, etc.

2) Results of Stage 1: For determining the optimal sizes of the batteries, the MILP ac-OPF problem formulation is solved [see (3)–(7), (10)–(16), and (19)–(22)], including the loads and PV scenarios and islanded mode of the system. Here, 3 h of islanding is considered in a day with equal probability (1/24) to the islanded scenarios. The total power balance for a day is shown in Fig. 7, and the obtained sizes of battery for the candidate buses are given in Table III. The load demand on bus 32 is more than three times the load demand on bus 17; therefore, the obtained rating of the battery on bus 32 is more than bus 17. This can relieve the minimum voltage constraint more effectively.

3) Stage 2: Life Cycle Analysis: The battery's performance is measured in terms of capacity, and the capacity degrades after a specific lifetime. So, it is not conclusive to analyze a battery's lifetime based only on the number of charging/discharging cycles, the DoD should also be looked upon. The DoD may vary, and there are no clearly defined standards of what constitutes a

TABLE IV
LIFETIME BASED ON DOD AND NUMBER OF CYCLES

Max. DoD(%)	Degradation per year(%)	Lifetime (years)	Predicted no. of cycles per day
Complete discharge cycles			
90	0.1413	7.07	1.16
80	0.1211	8.25	1.32
70	0.1248	8.007	1.69
Partial/fractional discharge cycles			
90	0.1185	8.46	0.97
80	0.1052	9.49	1.154
70	0.1207	8.28	0.992

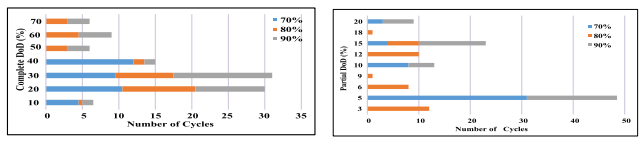

(a) (b)

Fig. 8. (a) Number of complete cycles. (b) Number of partial cycles for varying maximum DoD.

complete cycle. Furthermore, this article analyzes the lifetime based on discharge depth and the number of partial and full discharging cycles. It is observed that the determined optimal size of the battery remained the same on varying the upper limit of DoD from 70% to 90%. Also, there was a reduction in the number of discharging hours of the battery. For DoD values 60% and 50%, there was a change in the batteries' capacities at buses 32 and 33 and a voltage violation for DoD value 50%. The lifetime thus evaluated in years for three upper bounds of DoD values (90%, 80%, and 70%) with the counting of the complete and partial DoD according to the results obtained in stage 1 are given in Table IV.

Note that the lifetime is more and degradation is less when partial cycles are counted. The DoD value of 80% is selected as the most optimal value, and then the number of cycles was constrained using (24) to obtain the batteries' final optimal size. The number of cycles for partial and complete discharging cycles are shown in Fig. 8.

B. Test System B: Modified IIT Roorkee Distribution Network

The work is further extended to an Indian campus distribution network with reasonable modifications. Most of the buildings on the campus have rooftop solar penetrations with a total of 27 locations. When there is a low load in the system during summer vacations or lunchtime, there is an excess PV output, which can be utilized by integrating BESSs in the network. The IITR network has a total load capacity of 6 MW and a PV installed capacity of 1.8 MW, the single line diagram is shown in Fig. 9.

The voltage variations with and without storage integration at the nodes of the IITR distribution system are shown in Fig. 10(b). Note that the voltage variation is reduced to a small extent after the integration of storage at the bus 109. The energy and power rating of the battery hence calculated are given in Table V.

Authorized licensed use limited to: The University of Toronto. Downloaded on December 17,2022 at 09:05:05 UTC from IEEE Xplore. Restrictions apply.

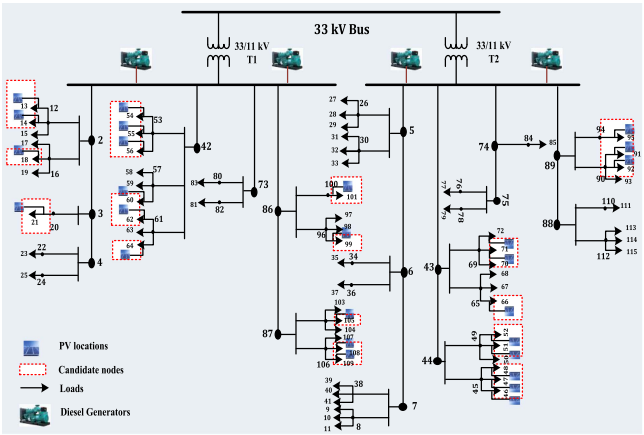

Fig. 9. Single line diagram of IITR distribution network with PV and DG locations.

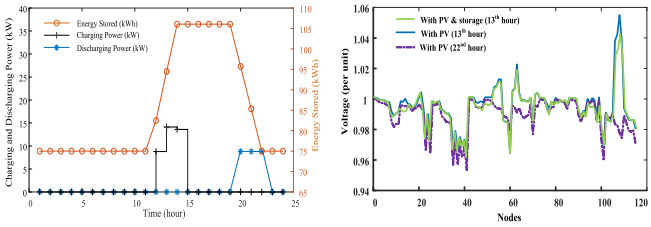

(a) (b)

Fig. 10. (a) Battery operating profile. (b) Voltage variation of the nodes with PV, without PV, and with storage and PV.

TABLE V
OBTAINED ENERGY AND POWER RATING

Bus no.	Energy rating (kWh)	Power rating (kW)
14	200	50
46	178	44.5
55	165	41.25
109	150	37.5

TABLE VI
OBTAINED ENERGY AND POWER RATING

Bus no.	Energy rating (MWh)	Power rating (MW)
49	10.6	2.65
77	6.17	1.54
85	2.113	0.52
87	4.52	1.13

C. Test System C: 141-Bus Radial Distribution System

To further test the scalability of the method, a standard 141-bus distribution network of Caracas is selected. All the data of the system including the locations of DGs are from [31]. The single line diagram of the system is shown in Fig. 11, and the obtained energy and power rating are given in Table VI.

The bus voltages are represented in the form of cumulative distribution function in Fig. 12(a). It is observed, more than 40% of the voltages are below 0.95 per unit for the base case. After battery integration, the voltages are improved. For a typical

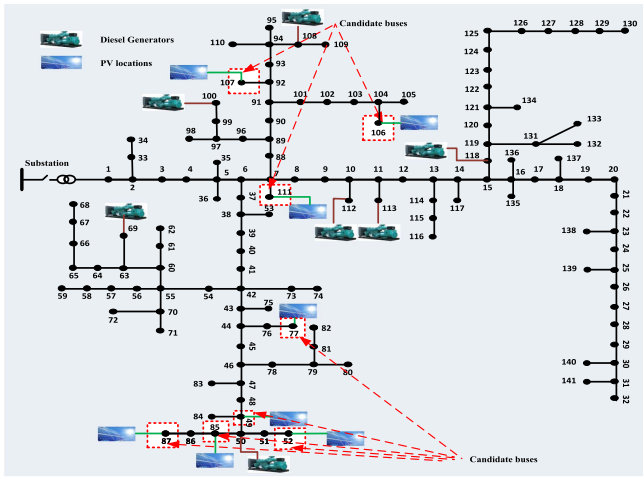

Fig. 11. Single line diagram of 141-bus distribution network with PV and DG locations.

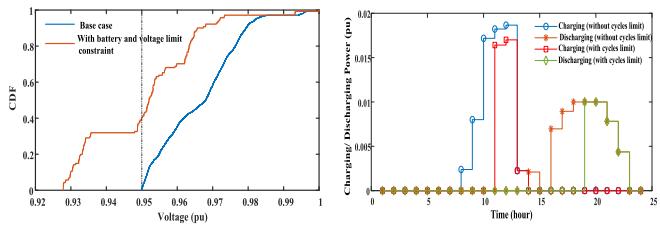

(a) (b)

Fig. 12. (a) Cumulative distribution of voltage variation for the base case and the battery-integrated system. (b) Battery operating profile with and without life cycle consideration.

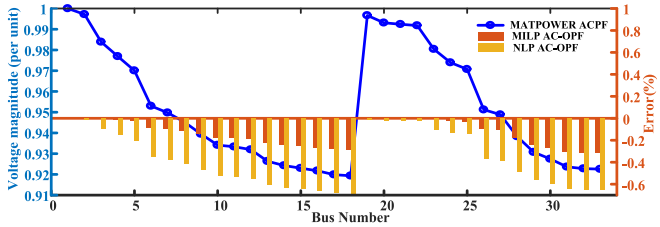

Fig. 13. Results of magnitude of bus voltage.

day, battery's charging and discharging periods are shown in Fig. 12(b), with and without life cycle consideration.

D. Verification Portfolio

1) Verification of Adopted Linearized Model With Benchmark: The ac-OPF formulation using YALMIP and GUROBI denoted as MILP ac-OPF is tested for accuracy with the MATPOWER results of the 33-bus distribution system, and the comparison is illustrated through the Fig. 13 and Table VII. An NLP method is also used for comparison of results, where losses are modeled as quadratic functions of real and reactive power flow and the error in voltage deviation is shown in Fig. 13. The

Authorized licensed use limited to: The University of Toronto. Downloaded on December 17,2022 at 09:05:05 UTC from IEEE Xplore. Restrictions apply.

TABLE VII
COMPARISON OF LOSSES AND GENERATED POWER INJECTIONS

Parameter	MATPOWER OPF	MILP AC-OPF	Relative error(%)
Real power injection(MW)	3.92	3.90	0.51
Reactive power injection(MVAR)	2.44	2.43	0.40
Real power loss(MW)	0.20	0.19	5
Reactive power loss(MVAR)	0.14	0.13	7.1

TABLE VIII
COMPARISON OF LOSSES AND GENERATED POWER INJECTIONS

Variables	Case A	Case B	Case C
Real and eactive power injection(MW and MVAR)	3.92 and 2.44	3.67 and 2.36	3.52 and 2.30
Investment Cost $	0	0	177304
Operation Cost $	0	19318	18956
Real and Reactive power loss(MW and MVAR)	0.203 and 0.14	0.40 and 0.30	0.15 and 0.12
Max. and Min. Voltage (pu)	0.997 and 0.91	1.061 and 0.958	1.05 and 0.95

maximum error in MILP formulation is -0.3% as compared to NLP error of -0.6% in case of voltage magnitude.

2) Numerical Results Verification: Considering the aforementioned data and assumptions, the proposed optimization problem has been solved for the following three cases.

a) *Case A:* With no renewable or diesel generator allocation.
b) *Case B:* Where PVs and diesel generators are added to the system.
c) *Case C:* With PV, DGs, and BESS.

The values of the most relevant variables are analyzed and given in Table VIII.

Case A is evaluated by forward–backward load flow as a base case without any DG. Here, the voltage deviation is very high. Therefore, case B is considered by adding PVs and diesel generators to improve the voltage profile and reduce the losses. Here, 80% of PV is proliferated, and the losses and voltages at nodes are increased. Therefore, we have proposed a method to improve the voltage profile and better utilize DGs. From the table, it is clear that the operation cost of the system is reduced with the allocation of ESSs in the distribution network. Moreover, there is a reduction in the losses, and the voltage profile is improved. Thus, the proposed method is verified for the energy storage allocation in an active distribution network. Moreover, the problem this article is formulated as MILP and solved using GUROBI solver in YALMIP-MATLAB interface. Hence, the mathematical optimization approach method guarantees the finest global optimal solution for convex problems and is robust for linear problems [1] and [4]. Therefore, the present research work solutions are near optimal global solutions. A comparative study is demonstrated in the subsequent section for further analysis of the method.

E. Comparative Studies

1) Comparison of Deterministic and Scenario-Based Planning: Since, uncertainty is a critical element in planning, a comparative study is performed for both systems in terms of deterministic and scenario-based planning methods for the grid-connected and 3 h (maximum limit with equal probability of islanding given to each hour during a day) of islanding mode of operation. As expected, Table IX gives that when the scenario variations are considered, the total capacity of the BESS is increased. Moreover, the computation time is increased due to the increase in the number of variables and the parameters.

TABLE IX
COMPARATIVE STUDY BASED ON SCENARIO PLANNING

Parameters	Deterministic	Scenarios
33-bus system		
Computation time	38.76 s	20,350 s
Best Objective value $	195900	1.328×10^6
Total Power losses	0.15 MW	0.16 MW
Total Energy and power rating	6.5 and 1.63 MW	8.00 and 2.00 MW
IITR distribution network		
Computation time	138.50 s	25,362 s
Best Objective value	157285	1.752×10^6
Total Power losses	45.7 kW	47.5 kW
Total Energy and power rating	496 and 124 kW	693 and 175 kW

2) Distributed BESS Placement: A comparison with the work given in [32] is made to establish the advantage of distributed BESS placement in the 33-bus distribution network. A 14.75-MWh BESS at bus 27 is proposed in [32] to control multiple services, such as losses and voltage regulation. However, this article proposes 8-MWh distributed BESSs installations to reduce losses, control the reverse power flow, and improve voltage profile. Moreover, if there is only one battery, wherever it is placed, the load at a nonselected bus will have more probability of isolation. On the other hand, several distributed batteries mean a lower probability that a load is isolated from the substation and the battery.

V. CONCLUSION

The integration of renewable energy resources necessitates the allocation of distributed energy storage to mitigate voltage deviation and defer distribution upgrades. This article illustrated a two-stage procedure for integrating lithium-ion batteries in a PV-penetrated active distribution network. The planning methodology considered an ac-OPF model with the uncertainty of PV and demand to determine the batteries' accurate size. Moreover, the reverse power flow due to excess PV penetration was utilized and the voltage was within limits after the integration of batteries in the system. The battery's life cycle was examined in the second stage with the partial cycle of discharge and complete discharge cycles. For lithium-ion batteries, partial cycle discharging was fine as there was no memory effect, and the battery does not need full discharges periodically. From the results, it was illustrated that with the partial cycle of discharge, the battery will last longer. Moreover, the method used here was the mathematical programming, which provides a robust solution, but may require significant computation time for large and complex problems. Also, the maximum discharging capacity of the battery gradually declined with its cycles, which can be kept as a future

Authorized licensed use limited to: The University of Toronto. Downloaded on December 17,2022 at 09:05:05 UTC from IEEE Xplore. Restrictions apply.

research direction. Furthermore, to enhance the stability and cost-effectiveness, a smart charging and discharging operation can be added to the problem. In addition, different types of DGs, such as wind, micro-turbines, and fuel cells, can be considered an extension to the OPF formulation.

REFERENCES

[1] B. Y. *et al.*, "Optimal sizing and placement of energy storage system in power grids: A state-of-the-art one-stop handbook," *J. Energy Storage*, vol. 32, 2020, Art. no. 101814.

[2] L. A. Wong, V. K. Ramachandaramurthy, P. Taylor, J. Ekanayake, S. L. Walker, and S. Padmanaban, "Review on the optimal placement, sizing and control of an energy storage system in the distribution network," *J. Energy Storage*, vol. 21, pp. 489–504, 2019.

[3] Central Electricity Authority, "Report on optimal generation capacity mix for 2029–2030," Central Electricity Authority, Ministry Power, Government India, New Delhi, India, Tech. Rep., Feb. 2019.

[4] S. A. Bozorgavari, J. Aghaei, S. Pirouzi, A. Nikoobakht, H. Farahmand, and M. Korpås, "Robust planning of distributed battery energy storage systems in flexible smart distribution networks: A comprehensive study," *Renew. Sustain. Energy Rev.*, vol. 123, 2020, Art. no. 109739.

[5] M. Nick, R. Cherkaoui, and M. Paolone, "Optimal planning of distributed energy storage systems in active distribution networks embedding grid reconfiguration," *IEEE Trans. Power Syst.*, vol. 33, no. 2, pp. 1577–1590, Mar. 2018.

[6] A. Giannitrapani, S. Paoletti, A. Vicino, and D. Zarrilli, "Optimal allocation of energy storage systems for voltage control in LV distribution networks," *IEEE Trans. Smart Grid*, vol. 8, no. 6, pp. 2859–2870, Nov. 2017.

[7] W. Lyzwa, M. Wierzbowski, and B. Olek, "MILP formulation for energy mix optimization," *IEEE Trans. Ind. Informat.*, vol. 11, no. 5, pp. 1166–1178, Oct. 2015.

[8] K. K. Mehmood, S. U. Khan, S. Lee, Z. M. Haider, M. K. Rafique, and C. Kim, "Optimal sizing and allocation of battery energy storage systems with wind and solar power DGS in a distribution network for voltage regulation considering the lifespan of batteries," *IET Renewable Power Gener.*, vol. 11, no. 10, pp. 1305–1315, 2017.

[9] B. Xu, A. Oudalov, A. Ulbig, G. Andersson, and D. S. Kirschen, "Modeling of lithium-ion battery degradation for cell life assessment," *IEEE Trans. Smart Grid*, vol. 9, no. 2, pp. 1131–1140, Mar. 2018.

[10] K. Antoniadou-Plytaria, D. Steen, L. A. Tuan, O. Carlson, and M. A. F. Ghazvini, "Market-based energy management model of a building microgrid considering battery degradation," *IEEE Trans. Smart Grid*, vol. 12, no. 2, pp. 1794–1804, Mar. 2020.

[11] J. Shen, S. Dusmez, and A. Khaligh, "Optimization of sizing and battery cycle life in battery/ultracapacitor hybrid energy storage systems for electric vehicle applications," *IEEE Trans. Ind. Informat.*, vol. 10, no. 4, pp. 2112–2121, Nov. 2014.

[12] S. de la Torre, J. M. González-González, J. A. Aguado, and S. Martín, "Optimal battery sizing considering degradation for renewable energy integration," *IET Renew. Power Gener.*, vol. 13, no. 4, pp. 572–577, 2019.

[13] G. Carpinelli, G. Celli, S. Mocci, F. Mottola, F. Pilo, and D. Proto, "Optimal integration of distributed energy storage devices in smart grids," *IEEE Trans. Smart Grid*, vol. 4, no. 2, pp. 985–995, Jun. 2013.

[14] H. Khorramdel, J. Aghaei, B. Khorramdel, and P. Siano, "Optimal battery sizing in microgrids using probabilistic unit commitment," *IEEE Trans. Ind. Informat.*, vol. 12, no. 2, pp. 834–843, Apr. 2016.

[15] S. F. Santos, D. Z. Fitiwi, M. Shafie-Khah, A. W. Bizuayehu, C. M. P. Cabrita, and J. P. S. Catalão, "New multistage and stochastic mathematical model for maximizing res hosting capacity–Part I: Problem formulation," *IEEE Trans. Sustain. Energy*, vol. 8, no. 1, pp. 304–319, Jan. 2017.

[16] M. Aien and M. Fotuhi-Firuzabad, "On possibilistic and probabilistic uncertainty assessment of power flow problem: A review and a new approach," *Renew. Sustain. Energy Rev.*, vol. 37, pp. 883–895, Sep. 2014.

[17] M. Jooshaki, H. Farzin, A. Abbaspour, M. Fotuhi-Firuzabad, and M. Lehtonen, "A model for stochastic planning of distribution network and autonomous DG units," *IEEE Trans. Ind. Informat.*, vol. 16, no. 6, pp. 3685–3696, Jun. 2020.

[18] A. Ehsan, M. Cheng, and Q. Yang, "Scenario-based planning of active distribution systems under uncertainties of renewable generation and electricity demand," *CSEE J. Power Energy Syst.*, vol. 5, no. 1, pp. 56–62, 2019.

[19] M. A. Awadallah and B. Venkatesh, "Energy storage in distribution system planning and operation: Current status and outstanding challenges," *Can. J. Elect. Comput. Eng.*, vol. 42, no. 1, pp. 10–19, 2019.

[20] M. A. Alotaibi and M. M. A. Salama, "An incentive-based multistage expansion planning model for smart distribution systems," *IEEE Trans. Power Syst.*, vol. 33, no. 5, pp. 5469–5485, Sep. 2018.

[21] *American National Standard for Electric Power Systems and Equipment-Voltage Ratings (60 hertz)*, ANSI Standard C84.1-2016, 2016.

[22] M. E. Baran and F. F. Wu, "Network reconfiguration in distribution systems for loss reduction and load balancing," *IEEE Trans. Power Del.*, vol. 4, no. 2, pp. 1401–1407, Apr. 1989.

[23] J. Lofberg, "YALMIP: A toolbox for modeling and optimization in matlab," in *Proc. IEEE Int. Conf. Robot. Automat.*, 2004, pp. 284–289.

[24] A. Feinberg and A. Widom, "Thermodynamic extensions of Miner's rule to chemical cells," in *Proc. Annu. Rel. Maintainability Symp., Proc. Int. Symp. Product Qual. Integrity*, 2000, pp. 341–344.

[25] W. Cole and A. W. Frazier, "Cost projections for utility-scale battery storage: 2020 update," May 2020, doi: 10.2172/1665769.

[26] C. Grigg *et al.*, "The IEEE reliability test system-1996. A report prepared by the reliability test system task force of the application of probability methods subcommittee," *IEEE Trans. Power Syst.*, vol. 14, no. 3, pp. 1010–1020, Aug. 1999.

[27] M. Sengupta, Y. Xie, A. Lopez, A. Habte, G. Maclaurin, and J. Shelby, "The national solar radiation data base (NSRDB)," *Renewable Sustain. Energy Rev.*, vol. 89, pp. 51–60, 2018.

[28] S. Pineda and J. M. Morales, "Chronological time-period clustering for optimal capacity expansion planning with storage," *IEEE Trans. Power Syst.*, vol. 33, no. 6, pp. 7162–7170, Nov. 2018.

[29] S. Paul and N. P. Padhy, "Resilient scheduling portfolio of residential devices and plug-in electric vehicle by minimizing conditional value at risk," *IEEE Trans. Ind. Informat.*, vol. 15, no. 3, pp. 1566–1578, Mar. 2019.

[30] Y. Wu, M. Barati, and G. J. Lim, "A pool strategy of microgrid in power distribution electricity market," *IEEE Trans. Power Syst.*, vol. 35, no. 1, pp. 3–12, Jan. 2020.

[31] B. Ahmadi, O. Ceylan, and A. Ozdemir, "Voltage profile improving and peak shaving using multi-type distributed generators and battery energy storage systems in distribution networks," in *Proc. 55th Int. Univ. Power Eng. Conf.*, 2020, pp. 1–6.

[32] N. Jayasekara, M. A. S. Masoum, and P. J. Wolfs, "Optimal operation of distributed energy storage systems to improve distribution network load and generation hosting capability," *IEEE Trans. Sustain. Energy*, vol. 7, no. 1, pp. 250–261, Jan. 2016.

Tripti Gangwar (Student Member, IEEE) received the B.Tech. degree in electrical and electronics engineering from the SRMS College of Engineering and Technology, Bareilly, India, in 2015, and the M.Tech. degree in power systems and control from the National Institute of Technology, Srinagar, India, in 2018. She is currently working toward the Ph.D. degree in planning and analysis of distributed energy storage in distribution networks with the Indian Institute of Technology Roorkee, Roorkee, India.

Her research interests include battery energy storage systems allocation, optimal power flow, and distributed energy resources integration in smart grids.

Ms. Gangwar was the recipient of the POSOCO Power System Award in 2019.

Authorized licensed use limited to: The University of Toronto. Downloaded on December 17,2022 at 09:05:05 UTC from IEEE Xplore. Restrictions apply.

Narayana Prasad Padhy (Senior Member, IEEE) received the Ph.D. degree in power systems engineering from Anna University, Chennai, India, in 1997.

He is currently a Professor (HAG) with the Department of Electrical Engineering, Indian Institute of Technology (IIT) Roorkee, Roorkee, India, the Director of the Malaviya National Institute of Technology, Jaipur, India, and the Mentor Director of the Indian Institute of Information Technology Kota. He is also the National lead of many national and international projects, such as DSIDES, ID-EDGe, and HEAPD, and part of other international projects, namely Indo-US UI-ASSIST and Indo U.K. ZED-I. Earlier, he was the Dean of Academic Affairs, Institute, NEEPCO, 92 Batch, and Ravi Mohan Mangal Institute Chair Professors, IIT Roorkee. He has authored or coauthored more than 200 research articles in reputed international journals and conference proceedings. His research interests include power system analysis, demand side management, energy market, network pricing, ac–dc smart grid, and application of machine learning techniques in power systems.

Dr. Padhy is a Fellow of the Indian National Academy of Engineers, the Institution of Electronics and Telecommunication Engineers, India, the Institution of Engineering and Technology, and the Institution of Engineers and India. He was the recipient of the IEEE PES Outstanding Engineers Award 2018, and the Boyscast Fellowship and the Humboldt Experienced research Fellowship, in 2005 and 2009, respectively.

Premalata Jena (Senior Member, IEEE) received the B.Tech. degree in electrical engineering from Utkal University, Odisha, India, in 2001, and the M.Tech. and Ph.D. degrees in power system engineering from the Department of Electrical Engineering, Indian Institute of Technology (IIT) Kharagpur, Kharagpur, India, in 2006 and 2011, respectively.

Since 2012, she has been an Assistant Professor with the Department of Electrical Engineering, IIT Roorkee, Roorkee, India, where she is currently an Associate Professor with the Department of Electrical Engineering. Her research interests include power system protection, microgrid protection, and issues due to the integration of renewables with the existing power grid.

Dr. Jena was the recipient of the SERB-POWER Fellowship-2022 from SERB, New Delhi, the Women Excellence Award-2017 from DST, New Delhi, the Young Engineer Award, Indian National Academy of Engineering, and the POSOCO Power System Award, Power Grid Corporation of India Ltd., India, in 2013.

Authorized licensed use limited to: The University of Toronto. Downloaded on December 17,2022 at 09:05:05 UTC from IEEE Xplore. Restrictions apply.